

Search for E6 isosinglet quarks in ATLAS

2nd December 2024

R. Mehdiyev^{1,2}, S. Sultansoy^{2,3}, G. Unel^{4,5}, M. Yilmaz³

Abstract

We consider pair production of new down-type isosinglet quarks originating from E_6 , favorite gauge symmetry group in superstring inspired GUT models. The study concentrates on the possibility of observing the lightest of the new quarks in the ATLAS detector at the forthcoming LHC accelerator, using the $ZZjj$ decay channel. Both signal and background events are studied using tree level event generators based on Monte Carlo techniques. The detector effects are taken into account using the ATLAS fast simulation tool, ATLFAST. Although the analysis cuts were optimized for a D quark mass of 800 GeV, other D quark mass values, from 600 up to 1200 GeV have also been considered. It is shown that ATLAS will discover the D quark within the first year of low luminosity LHC operation if its mass is less than 650 GeV. For the case of two years of full luminosity running, the five sigma discovery reach is about 1 TeV.

1 Introduction

If observed, the long awaited discovery of the Higgs particle at the LHC experiments [1, 2] will complete the validation of the basic principles of the Standard Model (SM). However, the well known deficiencies of the SM, such as the arbitrariness of the fermion mass spectrum and mixings, the number of families, the real unification of the fundamental interactions and the origin of baryon asymmetry of the universe require extensions of the SM to achieve more complete theories. In general, these extensions predict the existence of new fundamental particles and interactions. The forthcoming LHC will give the opportunity to explore new colored particles and their interactions to test these predictions. Three types of new quarks (see [3] for general classification) are of special interest: the fourth SM family quarks, up type and down type weak isosinglet quarks. The existence of the fourth SM family is favored by flavor democracy (see [4] and references therein for details), $Q=2/3$ quarks are predicted by the little Higgs model [5] and $Q = -1/3$ isosinglet quarks are predicted by Grand Unification Theories (GUTs), with E_6 as the unification group [6]. The GUT models permit solving at least two of above mentioned problems, namely, the complete unification of the fundamental interactions (except gravity) and baryon asymmetry of the observed universe by merging strong and electroweak interactions in a single gauge group. Theories adding gravity to the unification of fundamental forces, superstring and supergravity theories [7] also favor E_6 as a gauge symmetry group when compactified from 10 (or 11) dimensions down to 3+1 that we observe. (see [8] and references therein for a review of E_6 GUTs).

For LHC, the production and observation of the first and second type of new quarks has been investigated in [1, 9] and [10] respectively. In this work, we study the possibility to observe the third, down type isosinglet quarks predicted by the E_6 -GUT model, at LHC in general, and, specifically in the ATLAS experiment[1]. The current experimental limit on the mass of isosinglet quark is $m > 199$ GeV [11]. The detailed study for down type isosinglet quark signatures at Tevatron has been recently performed in [12] and it has been shown that the upgraded Tevatron would allow a mass reach up to about 300 GeV.

¹Université de Montréal, Département de Physique, Montréal, Canada.

²Institute of Physics, Academy of Sciences, Baku, Azerbaijan.

³Gazi University, Physics Department, Ankara, Turkey.

⁴CERN, Physics Department, Geneva, Switzerland.

⁵University of California at Irvine, Physics Department, USA.

2 The Model

If the origins of the SM $SU_C(3) \times SU_W(2) \times U_Y(1)$ structure are from the breaking of the E_6 GUT scale down to the electroweak scale, then the quark sector of SM is extended in the following manner:

$$\begin{pmatrix} u_L \\ d_L \end{pmatrix}, u_R, d_R, D_L, D_R; \quad \begin{pmatrix} c_L \\ s_L \end{pmatrix}, c_R, s_R, S_L, S_R; \quad \begin{pmatrix} t_L \\ b_L \end{pmatrix}, t_R, b_R, B_L, B_R. \quad (1)$$

As shown, each SM family is extended by the addition of an isosinglet quark. The new quarks are denoted by letters D , S , and B . The mixings between these and SM down type quarks is responsible for the decays of the new quarks.

These mixings increase the number of observable angles (N_Θ) and phases (N_Φ) with respect to the SM CKM matrix. For a general multi-quark model, one has [13] :

$$\begin{aligned} N_\Theta &= N \times \left(l + m - \frac{3N + 1}{2} \right) \\ N_\Phi &= (N - 1) \times \left(l + m - \frac{3N + 2}{2} \right) \end{aligned} \quad (2)$$

where l and m are the numbers of the up-type and down-type quarks respectively; and N is the number of $SU(2)_W$ doublets formed by left handed quarks. In the case of E_6 model, we have $m = 2l = 2N = 6$ and Eq. (2) yields $N_\Theta = 12$ and $N_\Phi = 7$. The special case $m = l + 1 = N + 1 = 4$, considered in [12], yields $N_\Theta = 6$ and $N_\Phi = 3$ which coincides with the number of parameters in the Little Higgs models with one additional isosinglet up-type quark [5].

In this study, the intrafamily mixings of the new quarks are assumed to be dominant with respect to their inter-family mixings. In addition, similar to the SM hierarchy, the D quark is taken to be the lightest one. The usual CKM mixings, represented by superscript θ , are taken to be in the up sector for simplicity of calculation (which does not affect the results). Therefore, the Lagrangian responsible for the decay of D quark becomes [14] :

$$\begin{aligned} \mathcal{L}_D &= \frac{\sqrt{4\pi\alpha_{em}}}{2\sqrt{2}\sin\theta_W} \left[\bar{u}^\theta \gamma_\alpha (1 - \gamma_5) d \cos\phi + \bar{u}^\theta \gamma_\alpha (1 - \gamma_5) D \sin\phi \right] W^\alpha \\ &- \frac{\sqrt{4\pi\alpha_{em}}}{4\sin\theta_W} \left[\frac{\sin\phi \cos\phi}{\cos\theta_W} \bar{d} \gamma_\alpha (1 - \gamma_5) D \right] Z^\alpha + h.c. \end{aligned} \quad (3)$$

The measured values of V_{ud}, V_{us}, V_{ub} constrain the d and D mixing angle ϕ to $\sin\phi \leq 0.07$ assuming unitarity of the 4×4 CKM matrix [11]. The total decay width and the contribution by neutral and charged currents were already estimated in [14]. As reported in this work, the D quark decays through a W boson with a branching ratio of 67% and through a Z boson with a branching ratio of 33%. The total width of the D quark as a function of its mass is shown in Fig. 1 for the illustrative value of $\sin\phi = 0.05$. It is seen that the D quark has a rather narrow width and becomes even narrower with decreasing value of ϕ since it scales through a $\sin^2\phi$ dependence.

This study will concentrate on the pair production of the D quarks which is approximately independent of the value of $\sin\phi$. One should note that the additional consideration of single production of D quark increases the overall D quark production rate; for example by about 40% for $m_D = 800$ GeV. However, final state particles and SM backgrounds are different from the pair production case, making it a rather different process to study.

3 Pair Production at LHC - signal at generator level

The main tree level Feynman diagrams for the pair production of D quarks at LHC are presented in Fig. 2. The $gD\bar{D}$ and $\gamma D\bar{D}$ vertices are the same as their SM down quark counterparts. The modification to the $ZD\bar{D}$ vertex due to $d - D$ mixing can be neglected due to small value of $\sin\phi$.

Figure 1: The width of D quark as a function of its mass ($\sin \phi = 0.05$)

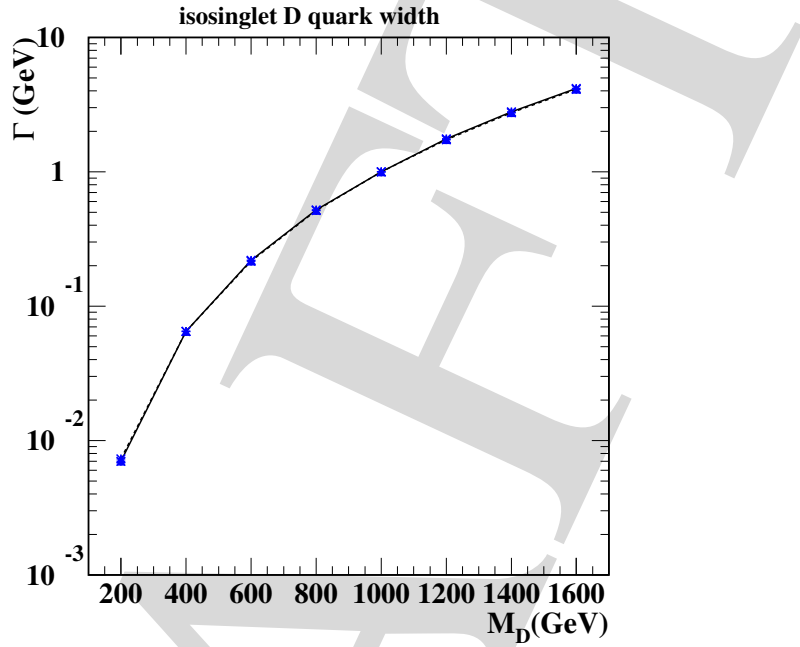


Figure 2: The tree level Feynman diagrams for the pair production of isosinglet quarks

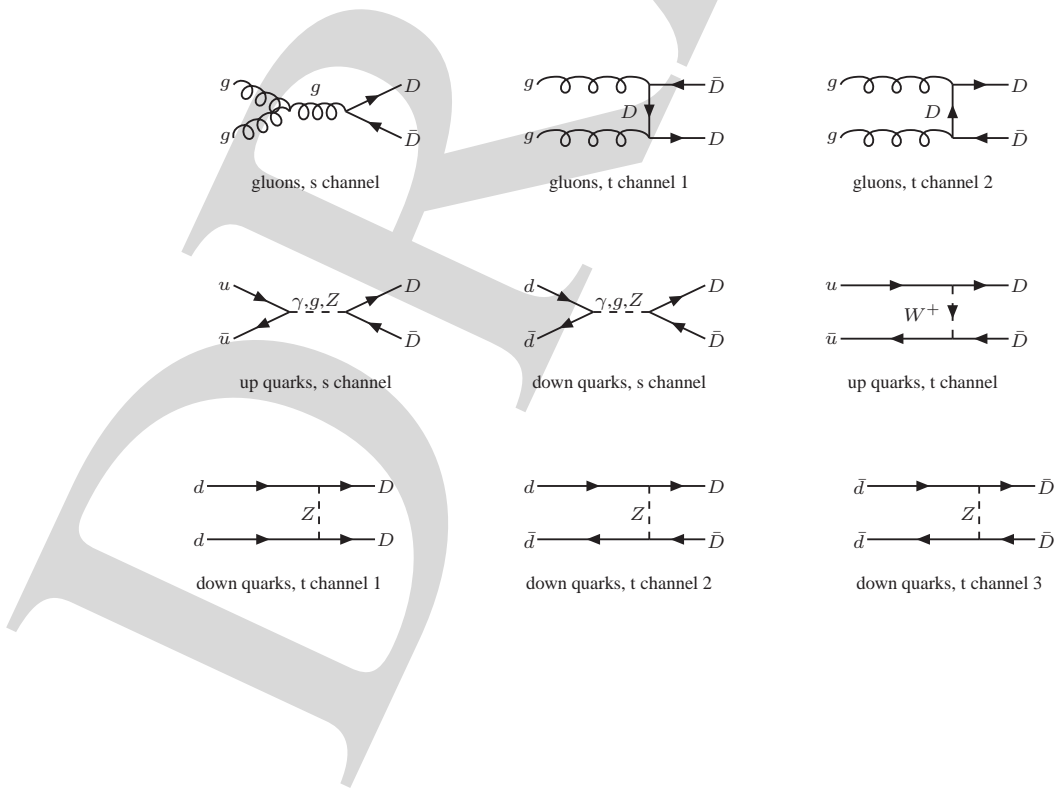
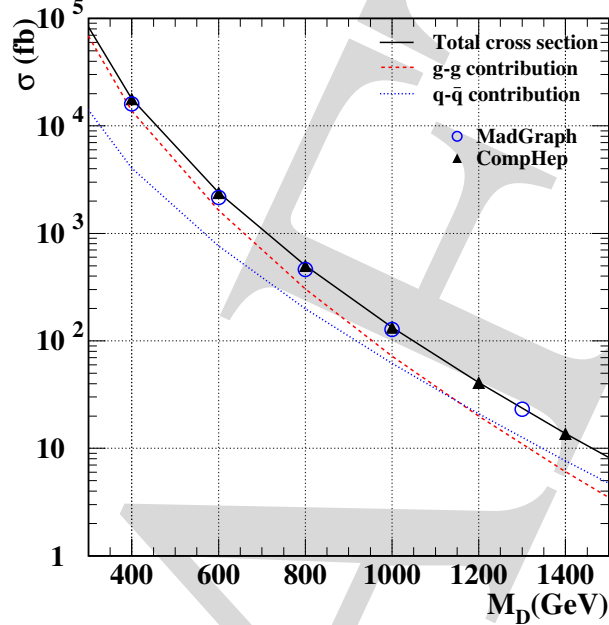


Figure 3: The $D\bar{D}$ pair total production cross section (solid line) as a function of D quark mass is shown as calculated with CompHep (triangles) and with MadGraph (circles). The dashed line is for the gluon contribution and the dotted line is for the quark contribution. The two generators agree within 2% and the effect of PDF uncertainties is computed to be less than 10% through 5 orders of magnitude in the cross section.



The Lagrangian in Eq. (3) was implemented into tree level event generators, *Comphep* [15] version 4.3 and *Madgraph* [16] version 2.3. The total pair production cross sections from these two Monte Carlo generators are shown in Fig. 3. The difference in cross section calculated by these two generators, the first one, based on full matrix element calculation and other on the numerical methods is less than 5% for the range of D quark mass from 400 to 1400 GeV. The impact of uncertainties in parton distribution functions (PDFs) [17], is calculated by using different PDF sets, to be less than 10% for the same range. For example at $m_D = 800$ GeV, the cross section values are 450 (CompHep, CTEQ6L1), 468 (CompHep, CTEQ5L) and 449 (MadGraph, CTEQ6L1), 459 (MadGraph, CTEQ5L) fb with an error of about one percent. The same figure also contains the partial (gg and $q\bar{q}$) contributions showing that the largest contribution to the total cross section comes from the first three diagrams for D quark masses < 1100 GeV, while for higher D quark masses, contributions from s -channel $q\bar{q}$ subprocesses becomes dominant. The t -channel diagrams mediated by Z and W bosons, shown on the bottom row of Fig. 2, which are suppressed by the small value of $\sin \phi$ (for example 0.4 fb at $m_D = 800$ GeV) are also included in the signal generation.

The isosinglet quarks being too heavy are expected to immediately decay into SM particles. The possible decay channels for the D quark pairs are summarized in Table 1. We have initially focused on the 4 lepton final states of the neutral channel only: although it has the smallest branching ratio, the possibility of reconstructing the invariant mass for Z bosons and thus for both D quarks makes it favorable for a feasibility study. Therefore the final state we would be looking for is composed of two high transverse momenta jets and two Z bosons, all coming from the decay of the D quarks. The high transverse momentum of the jets coming from the D quark decays can be used to distinguish the signal events from the background. All the SM processes allowed in proton collisions yielding two Z bosons and two jets (originating from any parton except b and t quarks) were considered as background. These can be classified in three categories via the initial state partons: $q\bar{q}$, qg and gg where g stands for gluon and q can be any quark or anti-quark from the first two families. Although a complete list can be seen in [18], one should note that the 70% of the background cross section originates from the processes in first two categories: $qg \rightarrow qgZZ$ (where $q = u, d, \bar{d}$) contributes 58%, and $d\bar{d} \rightarrow ggZZ$ contributes 12%.

Table 1: The possible signal channels. The fourth column contains the branching ratios of the SM particles, whereas the last column has the total branching ratios.

| $D\bar{D} \rightarrow$ | Final State | Expected Signal | Decay B.R. | Total B.R. |
|-----------------------------|---|----------------------------|----------------------------|------------|
| 0.33×0.33 | $Z \rightarrow l\bar{l} Z \rightarrow l\bar{l}$ | $4l + 2jet$ | 0.07×0.07 | 0.0005 |
| | $Z \rightarrow l\bar{l} Z \rightarrow vv$ | $2l + 2jet + \cancel{E}_T$ | $2 \times 0.07 \times 0.2$ | 0.0028 |
| | $Z \rightarrow l\bar{l} Z \rightarrow q\bar{q}$ | $2l + 4jet$ | $2 \times 0.07 \times 0.7$ | 0.0107 |
| $2 \times 0.33 \times 0.67$ | $Z \rightarrow l\bar{l} W \rightarrow l\bar{v}$ | $3l + 2jet + \cancel{E}_T$ | 0.07×0.21 | 0.0065 |
| | $Z \rightarrow l\bar{l} W \rightarrow q\bar{q}$ | $2l + 4jet$ | 0.07×0.68 | 0.0211 |

The simple requirements imposed at the generator level are:

$$\begin{aligned}
 |\eta_p| &< 2.5, \\
 P_{T,p} &> 100 \text{ GeV}, \\
 R_{p\bar{p}} &> 0.4, \\
 |\eta_Z| &< 5.0
 \end{aligned} \tag{4}$$

where R is the cone separation angle between two partons ($p = d, \bar{d}$), η_p and η_Z are pseudorapidities of a parton and Z boson respectively, and $P_{T,p}$ is the parton transverse momentum. Selection of η region is driven by partonic spectra pseudorapidity distributions, which are peaked in the barrel detector area. The signal cross section was calculated in both generators as a function of D quark mass, but the background only in Madgraph as it is faster in numerical evaluation. For $m_D = 800$ GeV, using the generator level cuts listed in Eq. (4), the cross section of the ZZ 2jet channel is found as $\sigma_{signal} = 45.4 \pm 2$ fb (CompHep) whereas the SM background for the same final state particles as $\sigma_{bg} = 345 \pm 17$ fb (MadGraph). Already at this level, a significance of $S/\sqrt{B} \approx 2.4$ can be obtained with an integrated luminosity of 1 fb^{-1} .

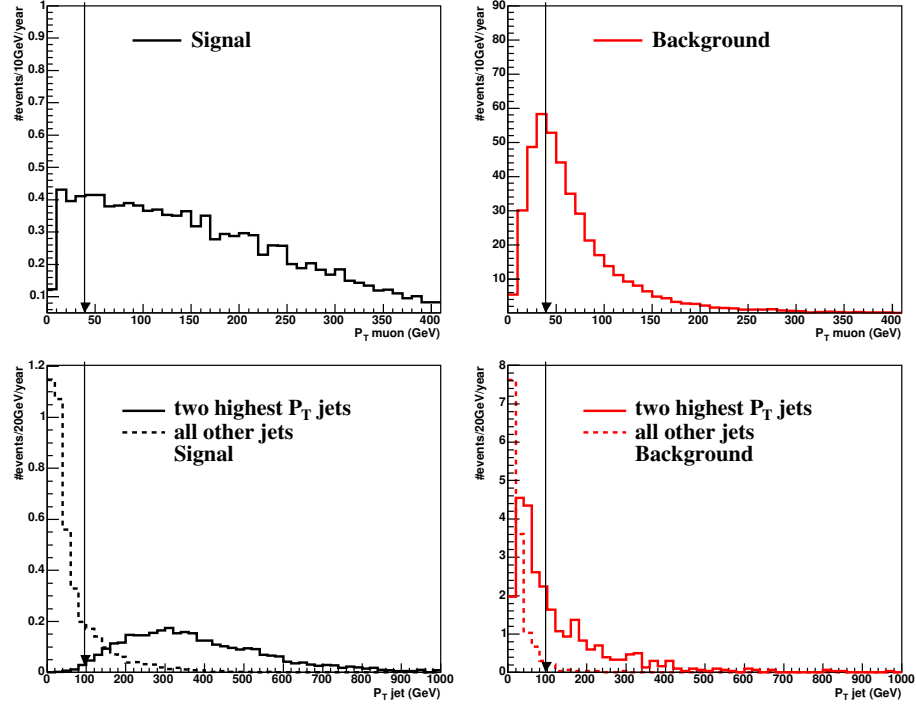
4 Observation in ATLAS detector using $4l$ 2jet channel

Using the cuts listed in the previous section, 5000 signal events at $m_D = 800$ GeV in CompHep and slightly relaxing the jet transverse momentum cut, ($P_{T,j} > 50$ GeV), 40000 background events in MadGraph were generated. The D quarks in signal events were made to decay in CompHep into SM particles. The final state particles for both signal and background events were fed into *Pythia* version 6.218 [19] for initial and final state radiation, as well as, hadronization using the CompHep-*Pythia* and MadGraph-*Pythia* interfaces provided by Athena (the ATLAS offline software framework) v9.0.3. To incorporate the detector effects, all event samples were processed through the ATLAS fast simulation tool, ATLFast [20], and the final analysis has been done using physics objects that it provided.

It must be noted that ATLFast uses a parameterization for electrons, muons and hadrons without the detailed simulation of showers in the calorimeters. There is also a separate parameterization on the resolution for muons and electron tracks for the inner detector efficiencies. Minimum transverse energy of electromagnetic and hadronic clusters to be considered as electron or jet showers are $E_T > 5$ GeV and $E_T > 10$ GeV, respectively. Electromagnetic and hadronic cells in ATLFast have the same granularity: $\Delta\eta \times \Delta\phi = 0.1 \times 0.1$. The electron isolation criteria requires a minimum distance $\Delta R \equiv \sqrt{(\Delta\eta)^2 + (\Delta\phi)^2} \geq 0.4$ from other clusters and a maximum transverse energy deposition, $E_T < 10$ GeV in outer cells accompanying the electron candidate. These outer cells are to be in a cone of radius $\Delta R = 0.2$ along the direction of emission. Jets are reconstructed using the cone algorithm with the $\Delta R = 0.4$ cone size. The smearing of particle clusters and jets, their calibration is tuned to what is expected for the performance of the ATLAS detector from full simulation and reconstruction using the GEANT package[21].

For this initial feasibility study, where the aim is to reconstruct the invariant mass of both D quarks, only e and μ decays of Z bosons are considered. Although the effective cross section becomes small compared to other decay channels, the benefits of this selection for a clean signal and for correct invariant mass reconstruction are indisputable. Other studies involving the invisible decays of Z boson and leptonic decays of W boson are in preparation. For the initial state particles,

Figure 4: The transverse momentum cuts for muons (upper set) and jets (lower set). The plots for signal at $M_D = 800$ GeV and the SM backgrounds are shown with arrows pointing at the cut values. The highest jet P_T for signal events peaks around 300 GeV, whereas for background no such peak is observed.



gg , $u\bar{u}$ and $d\bar{d}$ sub-channels were studied separately, and for final state particles only light quark jets were considered. The misidentification effects were omitted, the used PDF was CTEQ6L1 [17]. For the case of $M_D = 800$ GeV, the contributions from each sub-channel to the final cross section were about 50 %, 32% and 18% respectively.

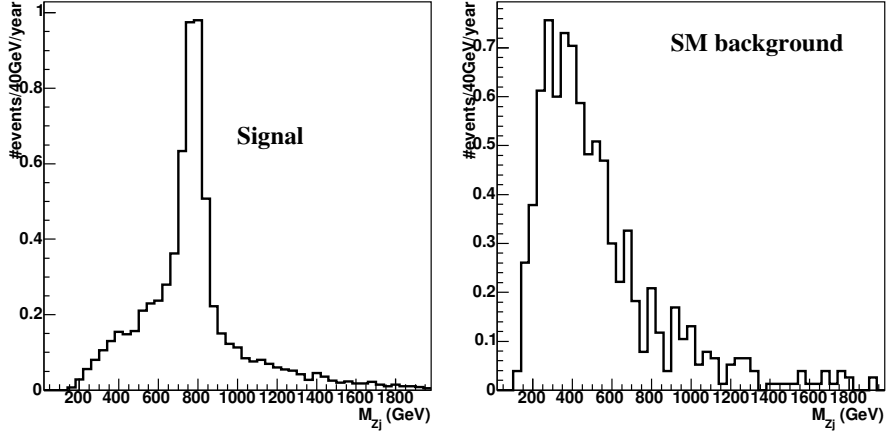
4.1 Both $Z \rightarrow \mu\mu$ case

To reconstruct the Z boson, high P_T isolated muons were required. The efficiency of finding 4 isolated muons to reconstruct the two initial Z bosons is roughly 50%. The percentage of muons surviving the transverse momentum cut in equation 5 is about 87%. The events with at least two jets of transverse momenta greater than 100 GeV were kept. The muon and jet momentum distributions and the imposed cuts for different input channels can be seen in Fig. 4. In the lower plots, the solid line shows the momenta of the two most energetic jets, whereas the dashed curve is for all other jets. In all sets, the arrow points to the imposed cut value. The efficiency of reconstructing two Z bosons from the four isolated muons is about 90% for a mass window around 90 GeV. The correct association of the two selected jets to the two reconstructed Z bosons is not known and involves combinatorics. This problem is partially solved by requesting the absolute value of the invariant mass difference between their possible combinations to be smaller than a fixed value, 400 GeV. The Fig. 5 contains the reconstructed invariant masses of the D quarks using this cut for both signal and background events. The effect of wrong association has the impact of enlarging the tails for the signal invariant mass distribution.

All of the analysis level cuts are listed below :

$$\begin{aligned}
 N_\mu &= 4, \\
 P_{T,\mu} &> 40 \text{ GeV}, \\
 M_Z &= 90 \pm 20 \text{ GeV},
 \end{aligned} \tag{5}$$

Figure 5: The invariant mass plots for signal at $M_D = 800$ GeV and background events in the $Z \rightarrow \mu\mu$ case, obtained from two reconstructed Z bosons and two highest P_T jets.



$$\begin{aligned}
 N_{jet} &\geq 2, \\
 P_{T,jet} &\geq 100 \text{ GeV}, \\
 |M_{D1} - M_{D2}| &< 400 \text{ GeV}.
 \end{aligned}$$

The selection cut efficiencies are given in Table 2. The background events were processed using the same cuts and the resulting invariant mass plots are shown in Fig. 5.

Table 2: The individual selection cut efficiencies in percent for the both $Z \rightarrow \mu\mu$ case, for signal and background

| channel | N_μ | M_Z | $P_{T,\mu}$ | N_{jet} | $P_{T,jet}$ | $M_{D1} - M_{D2}$ | $\epsilon_{combined}$ |
|------------|---------|-------|-------------|-----------|-------------|-------------------|-----------------------|
| Signal | 48 | 91 | 59 | 100 | 95 | 94 | 23 |
| Background | 34 | 96 | 16 | 96 | 12 | 11 | 0.07 |

4.2 Both $Z \rightarrow ee$ case

The cuts in this channel are same as the cuts in Eq. (5), except the cut on the transverse momentum of electron, $P_{T,e} > 15$ GeV has been used. The selection cut efficiencies for this case are shown in Table 3 for both signal and background. The electron cuts leave slightly higher surviving events for both signal and background. The invariant mass spectrum obtained for the D quark is given in Fig. 6 for a bin width of 40 GeV, showing the expected number of signal events being larger than the background ones.

Table 3: The individual selection cut efficiencies in percent for the both $Z \rightarrow ee$ case for both signal and background.

| channel | N_e | M_Z | $P_{T,e}$ | N_{jet} | $P_{T,jet}$ | $M_{D1} - M_{D2}$ | $\epsilon_{combined}$ |
|------------|-------|-------|-----------|-----------|-------------|-------------------|-----------------------|
| Signal | 40 | 99 | 87 | 100 | 95 | 94 | 31 |
| Background | 37 | 98 | 83 | 94 | 7 | 9 | 0.2 |

Figure 6: The D quark invariant mass reconstruction in $Z \rightarrow ee$ case for all signal sub-channels as compared to SM background. The signal was generated for $M_D = 800$ GeV.

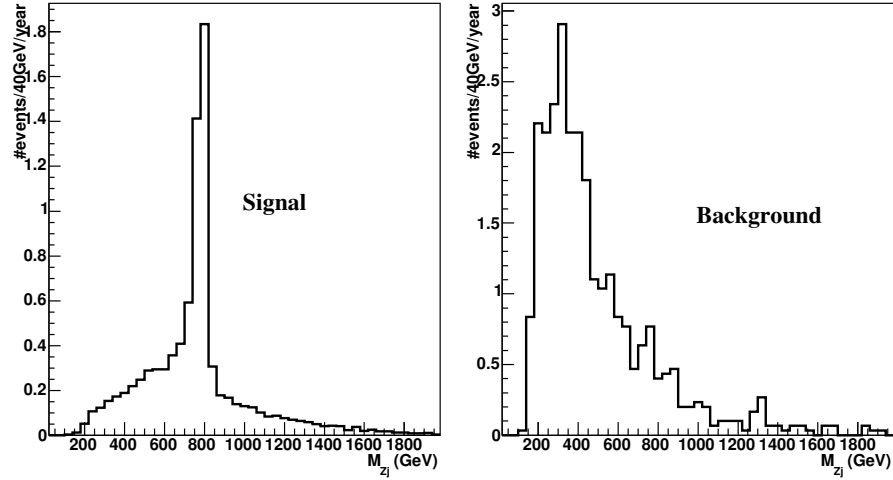
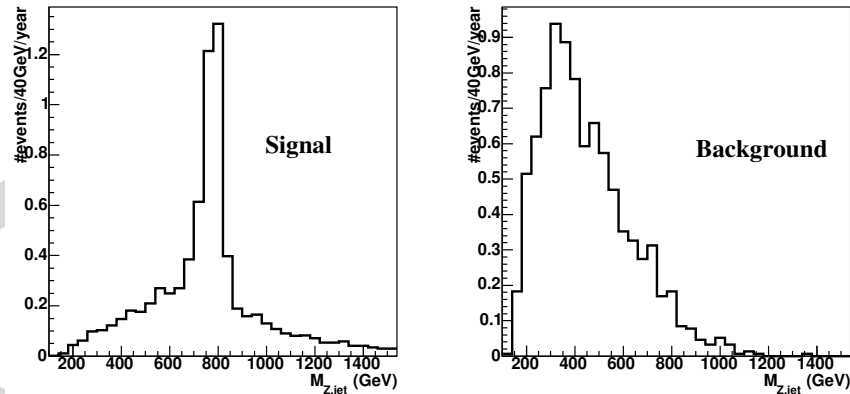


Figure 7: The D quark invariant mass reconstruction in $Z \rightarrow ee$ and $Z \rightarrow \mu\mu$ case for all signal sub-channels as compared to SM background. The signal was generated for $M_D = 800$ GeV.



4.3 One $Z \rightarrow ee$ and one $Z \rightarrow \mu\mu$ case

This case is based on two isolated electrons, two isolated muons and two jets. There is no ambiguity in the lepton selection for Z invariant mass reconstruction thus a simpler reconstruction algorithm suffices. This selection is summarized in the equation set 6:

$$\begin{aligned}
N_\mu &= 2, \quad N_e = 2, \\
P_{T,\mu} &> 40 \text{ GeV}, \\
P_{T,e} &> 15 \text{ GeV}, \\
N_{jet} &\geq 2 \\
P_{T,jet} &\geq 100 \text{ GeV}, \\
M_Z &= 90 \pm 20 \text{ GeV}, \\
|M_{D1} - M_{D2}| &< 400 \text{ GeV},
\end{aligned} \tag{6}$$

The selection cut efficiencies are given in Table 4. Since the branching ratio is higher by a factor of two, compared to first and second cases, this case yields more signal events and dominates the results. The reconstructed invariant mass for the signal and the SM background is given in Fig. 7 showing the expected number of signal events per year higher than the background ones.

Table 4: The individual selection cut efficiencies for one $Z \rightarrow ee$ and one $Z \rightarrow \mu\mu$ sub-case. The subscript l represents both electron and muon cases.

| channel | N_l | M_Z | $P_{T,l}$ | N_{jet} | $P_{T,jet}$ | $M_{D1} - M_{D2}$ | $\epsilon_{combined}$ |
|------------|-------|-------|-----------|-----------|-------------|-------------------|-----------------------|
| Signal | 44 | 94 | 71 | 100 | 93 | 94 | 26 |
| Background | 35 | 97 | 34 | 95 | 10 | 14 | 0.15 |

5 Results

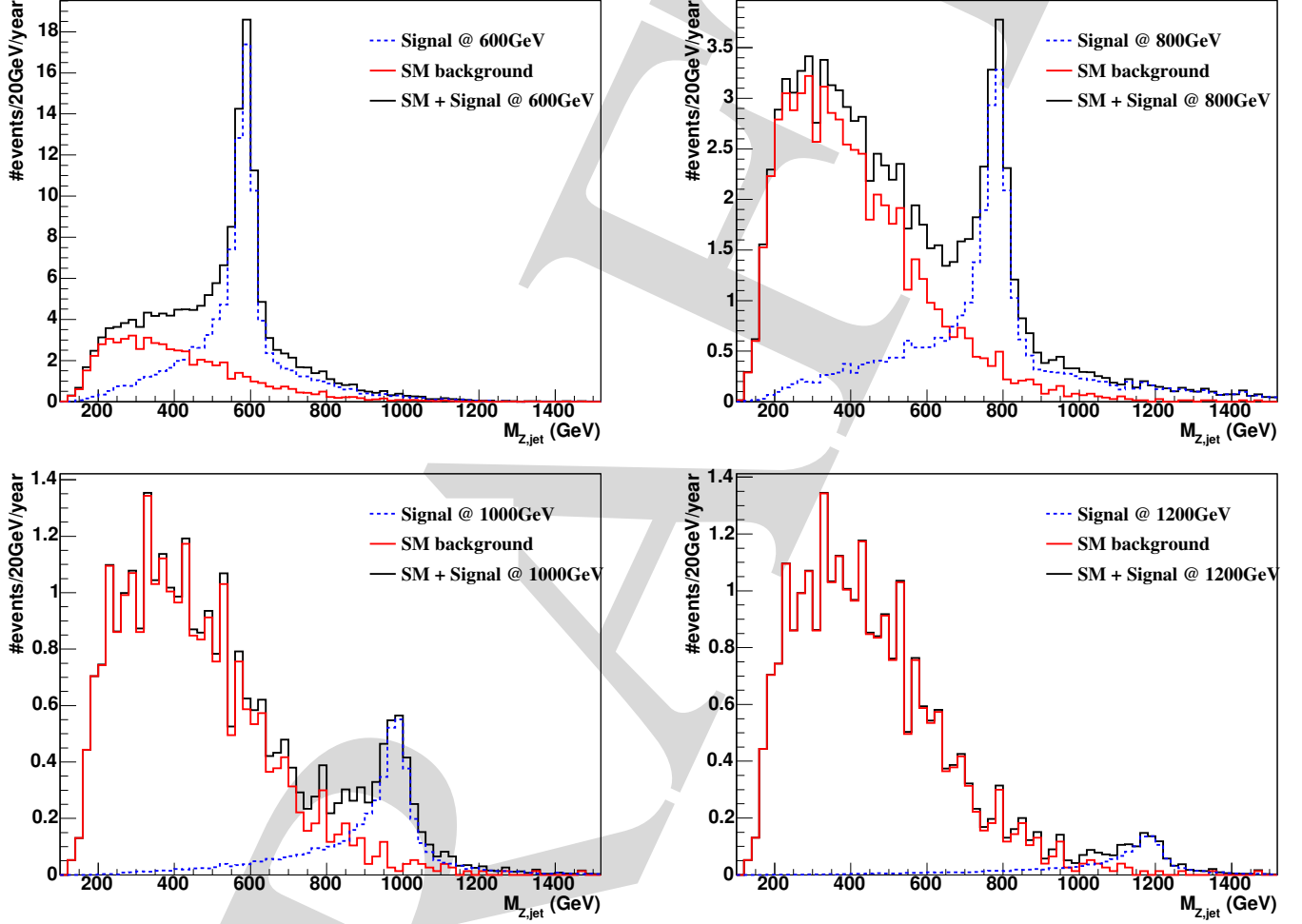
All three above mentioned leptonic reconstruction cases were considered for systematic studies at $M_D = 600, 800, 1000, 1200$ GeV. (The details of this analysis can be found in [18]) For values of D quark mass larger than 800 GeV, in order to increase the expected statistical significance of signal identification, the cuts on the basic kinematic variables are modified as:

$$\begin{aligned}
P_{T,\mu} &> 50 \text{ GeV}, \\
P_{T,e} &> 20 \text{ GeV}, \\
P_{T,jet} &> 120 \text{ GeV}.
\end{aligned} \tag{7}$$

Using the convention of defining a running accelerator year as 1×10^7 seconds, one LHC year at the full design luminosity corresponds to 100 fb^{-1} . For one such year worth of data, the signal events are compared to the SM background in Fig. 8. It is evident that for lowest of the considered masses, the leptonic channel gives an easy detection possibility, whereas for the highest mass case ($M_D=1200$ GeV) the signal is about the background level. If the Nature has assigned a high mass to the D quark, possible detection mechanisms would be either to tag one Z via its leptonic decays and consider the neutrino decays of the other, or would involve hadronic decays of at least one Z and methods to disentangle the jet association. The detailed study of these modes as well as the charged current decay modes is deferred to future work.

The expected signal significance for three years of nominal LHC luminosity run is shown in Fig. 9 left hand side. The significance is calculated at each mass point as S/\sqrt{B} where S and B are the number of accepted signal (S) and background (B) events in the selected mass window. For the mass window, the width is taken equal to $\pm 2\sigma$ from the

Figure 8: Combined results for possible signal observation at $M_D = 600, 800, 1000, 1200$ GeV and the relevant SM background are shown for 1 year of LHC at full luminosity. The dark line shows the signal and background added, the dashed line is for signal only and the light line shows the SM background.



Gaussian fit to the invariant mass distribution around the D peak. The shaded area in the same plot represents the statistical errors originating from the fact that a finite number of Monte Carlo events were generated. The statistical errors were calculated using binomial distribution and propagated to all significance and luminosity calculations. The reach of ATLAS to either exclude the existence of or discover the D quark using the dilepton channel is given in Table 5 for different D quark mass values. We observe that for $M_D = 600$ GeV, ATLAS could discover the D quark with a significance more than 5 sigma before the end of the first year low luminosity run. For $M_D = 1000$ GeV, about two and half years of high luminosity run are necessary for a 3 sigma signal observation claim. The graphical repreation is also given in Fig.9 right hand side. For these results, a possible source of systematic error is the selection of the QCD scale: although in a complete computation using all possible diagrams including loops this selection becomes irrelevant, this work relies on tree level calculations. An increase in QCD scale from the presently used value of Z boson mass up to D quark mass would mean a decrease in the total cross sections of about 65%. Such a change would also affect the results presented in this work, taking the 3 sigma signal observation limit mass from 1200 GeV down to 950 GeV for 3 years of high luminosity run.

Figure 9: On the left: the expected statistical significance after 3 years of running at nominal LHC luminosity; on the right: the integrated luminosities for 3 sigma observation and 5 sigma discovery cases as a function of D quark mass. The bands represent statistical uncertainties originating from finite MC sample size.

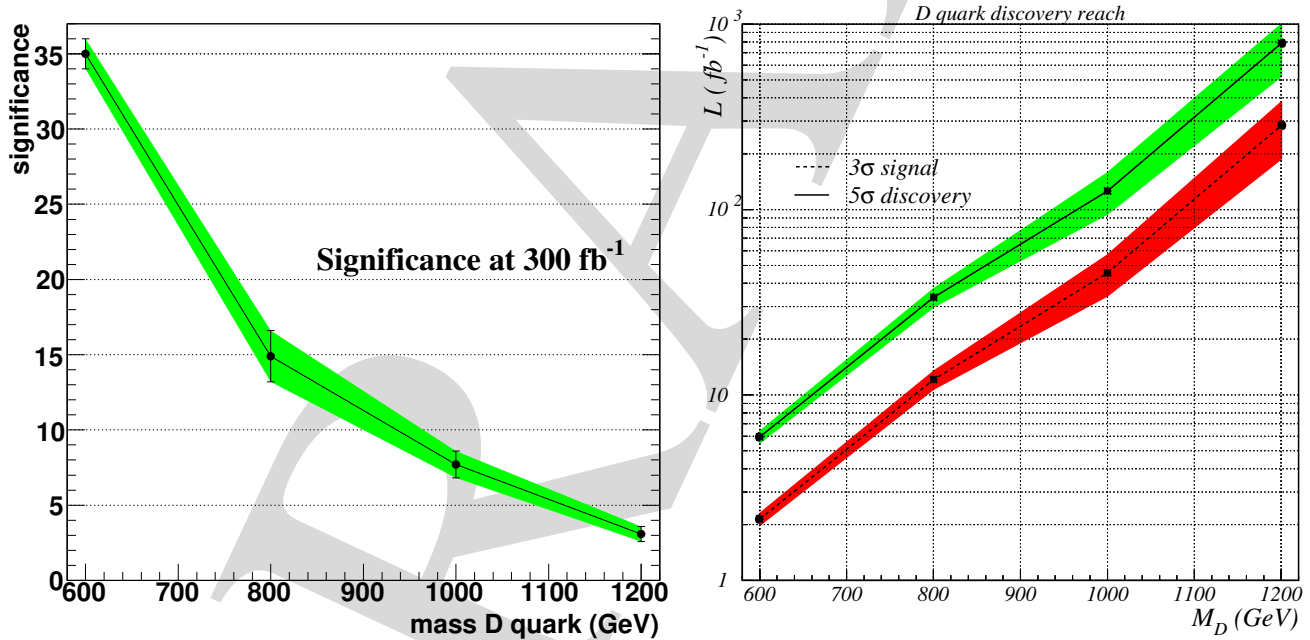


Table 5: The required integrated luminosity in fb^{-1} to either exclude or discover D quark as a function of its mass.

| D quark mass (GeV) | 600 | | 800 | | 1000 | | 1200 | |
|--|-------|------|-------|------|------|-------|-------|-------|
| signal & background events / year | 46.15 | 5.07 | 11.91 | 1.91 | 2.20 | 0.245 | 0.623 | 0.123 |
| Luminosity for 95% exclusion (fb^{-1}) | 0.96 | | 5.37 | | 20.2 | | 126 | |
| Luminosity for 3σ signal (fb^{-1}) | 2.14 | | 12.1 | | 45.6 | | 284 | |
| Luminosity for 5σ signal (fb^{-1}) | 5.95 | | 33.6 | | 126 | | 790 | |

6 Conclusions

Although the detector related backgrounds and the pile-up effects (which would be important at high luminosity LHC), are not considered in this work, this analysis shows that, for a range of D quark mass from 600 to 1000 GeV, ATLAS has a very strong discovery potential. The impact of the assumptions about D quark mass hierarchy and interfamily mixing is minimal: If the S quark is the lightest or the D quark mixes mostly to the second family, all the results and conclusions stay as they are. In case of the involvement of the third family, either via B quark being the lightest or via large mixings to the third quark family, the $b - jet$ tagging efficiencies should be convoluted with the presented results which would reduce the number of expected signal and background events by at least 50%.

To enlarge the experimental reach window for the higher D quark mass values, the inclusion of other channels (lines 2, 4 and 5 of the Table 1) is also envisaged. Furthermore, the inclusion of extra Z bosons predicted by the E_6 group could enhance the signal in the s channel if they have suitable masses. These studies are in preparation.

Acknowledgments

The authors would like to thank Louis Tremblet and CERN Micro Club for kindly providing computational facilities, and Georges Azuelos for useful discussions. R.M. would like to thank Alexander Belyaev for his assistance in model calculations. R.M. also thanks NSERC/Canada for their support. S.S and M.Y. acknowledge the support from the Turkish State Planning Committee under the contract DPT2002K-120250. G.U.'s work is supported in part by U.S. Department of Energy Grant DE FG0291ER40679. This work has been performed within the ATLAS Collaboration with the help of the simulation framework and tools which are the results of the collaboration-wide efforts.

References

- [1] ATLAS Detector and Physics Performance Technical Design Report. CERN/LHCC/99-14/15.
- [2] CMS collaboration, Technical proposal, CERN-LHCC-94-38.
- [3] P. H. Frampton, P. Q. Hung and M. Sher, Phys Rep. **330**, 263 (2000).
- [4] S. Sultansoy, hep-ph/0004271
- [5] N. Arkani-Hamed, A. G. Cohen and H. Georgi. Phys. Lett. B **513**, 232 (2001).
- [6] F. Gursey, P. Ramond and P. Sikivie, Phys. Lett. B **60**, 177 (1976); F. Gursey and M. Serdaroglu, Lett. Nuovo Cimento **21**, 28 (1978).
- [7] J.H. Schwarz, Lett. Math. Phys. **34** 309 (1995); E. Witten, Nucl. Phys. B **443** 85 (1995) .
- [8] J. Hewett and T. Rizzo, Phys. Rep. **183**, 193 (1989).
- [9] E. Arik et al., Phys.Rev.D **58**, 117701 (1998).

- [10] J.A. Aguilar-Saavedra, Phys.Lett.B **625**, 234 (2005).
- [11] S. Eidelmann et. al., P Phys. Lett. B **592**, 1 (2004).
- [12] T. C. Andre and C.L. Rosner, Phys. Rev. D. **69**, 035009, (2004).
- [13] Z. R. Babaev, V.S. Zamiralov and S.F. Sultanov, IHEP preprint, 81-88, Serpukhov, (1981).
- [14] O. Cakir and M. Yilmaz, Europhys. Lett. **38**, 13 (1997).
- [15] A. Pukhov, [arXiv:hep-ph/0412191]; E. Boos et al. [CompHEP Collaboration], Nucl. Instrum. Meth. A **534**, 250 (2004).
- [16] T. Stelzer and W. F. Long, Phys. Commun. **81**, 357 (1994).
- [17] J. Pumplin, D.R. Stump, J. Huston, H.L. Lai, P. Nadolsky and W.K. Tung, JHEP **0207**, 012 (2002) [arXiv:hep-ph/0201195].
- [18] R. Mehdiyev et al., ATL-PHYS-PUB-2005-021 (2005).
- [19] T. Sjostrand et al., Computer Phys. Commun. **135** (2001) 238 (LU TP 00-30, [hep-ph/0010017])
- [20] E. Richter-Was et al., ATLAS Note PHYS-98-131(1998); <http://www.hep.ucl.ac.uk/atlas/atlfast/>
- [21] S. Agostinelli et al., (Geant4 Collaboration), Nucl. Instrum. Meth. A **506**, 250 (2003).

